

# HIGH CURRENT LIMITATIONS FOR THE NSLS-II BOOSTER\*

A. Blednykh<sup>#</sup>, W. Cheng, R. P. Fliller, Y. Kawashima, J. Rose, T. Shaftan, L.-H. Yu.  
BNL, NSLS-II, Upton, NY, 11973-5000, U.S.A.

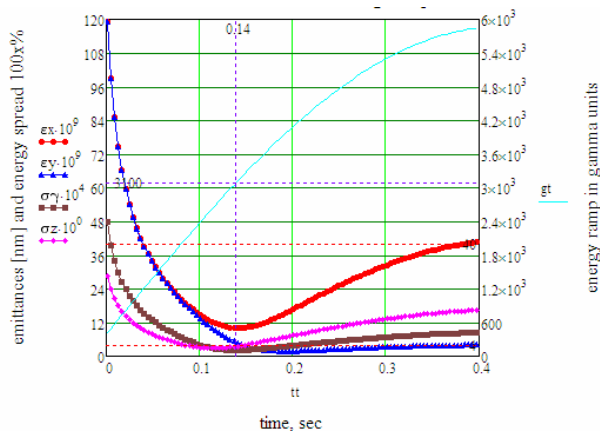
## Abstract

The NSLS-II booster has to provide high-current per bunch in order to support specialized bunch patterns in the NSLS-II storage ring required by user's community. To avoid high current limitations for the NSLS-II booster we studied instability thresholds, including the ion effects.

## INTRODUCTION

The NSLS-II booster [1] is required to produce a 3 GeV bunch train with an accelerated charge of about 10 nC at a repetition rate of 1 Hz and a horizontal beam emittance around 40 nm-rad. Injection into the booster ring takes place at an energy of 200 MeV. The booster magnetic field and RF voltage are ramped for 500 ms to accelerate the electron beam from the injection energy to the nominal energy of 3 GeV. At the maximum field of the ramp, the electron beam is extracted from the booster and injected into the main ring. The charge to be accelerated in the booster is 10 nC which corresponds to an average beam current of 20 mA.

In the Table 1 we present parameters for the NSLS-II booster. The NSLS-II booster has 500MHz RF and a revolution period of  $T_0=528\text{ns}$ . Short damping time ( $\tau_D=6\text{ms}$ ) at the maximum booster energy leads to a fully damped beam at the end of the ramp (Fig. 1). Here we assumed a sinusoidal ramp profile with the injection point "on the fly", i.e. on the rising slope of the energy ramp.



Initial values:  $E=200\text{ MeV}$ ,  $\epsilon_x=125\text{ nm}$ ,  $\epsilon_y=125\text{ nm}$ , energy spread=0.5%,  $bl=30\text{ ps}$   
Final values:  $E=3\text{ GeV}$ ,  $\epsilon_x=40\text{ nm}$ ,  $\epsilon_y=4\text{ nm}$ , energy spread=0.08%,  $bl=16\text{ ps}$

Figure 1: Beam parameters as functions of time along the energy ramp. Left vertical axis is in following units: horizontal ( $\epsilon_x$ , red dots) and vertical ( $\epsilon_y$ , blue triangles) emittances in  $\text{nm-rad}$ , energy spread ( $\sigma_\gamma/\gamma$ , brown squares) in 0.01%, bunch duration ( $\sigma_z$ , magenta diamonds) in  $\text{ps}$ . Right vertical axis is energy ramp in  $\gamma$ -units. Horizontal axis is time along the ramp.

\*Work supported by DOE contract DE-AC02-98CH10886.

<sup>#</sup>blednykh@bnl.gov

Table 1: NSLS-II Booster Parameters.

Circumference, m	158.4
Booster current, mA	20
Revolution time, ns	528
RF frequency, MHz	499.68
RF voltage, MV	1.2
Harmonic number	264
Emittance X/Y, nm	40/4
X/Y/Z tune	9.64/3.41/0.01
Momentum Compaction	0.0084
Energy loss per turn, keV	686
Damped energy spread, %	0.0082
Damped bunch length, mm	16.2

## RF SYSTEM

The 7-cell PETRA cavity will be installed in the NSLS-II booster tunnel to provide electron beam acceleration at 500MHz. The main instability effect can arise due to interaction of multi-bunched beam with electromagnetic fields of high order modes (HOM's) generated in the cavity structure (narrow band impedance). In order to avoid longitudinal and transverse coupled-bunch instabilities, HOM's have to be well damped. There is a concern that one of the damped HOM's in PETRA cavity can cause instabilities in the NSLS-II booster ring. To avoid possible beam current reduction the additional method of controlling HOM shunt impedance is implemented [2].

## INSTABILITY THRESHOLDS

We approximated that the basic profile of the NSLS-II booster vacuum chamber by a round cross-section with radii  $d=25\text{mm}$  and  $b=12.5\text{mm}$  in the region of straight and arc sections respectively. The straight section length is 8.6m. The arc length is 31m. The NSLS-II booster vacuum chamber can be presented as a sum of four step transitions (Fig. 2) with a length of  $g=31\text{m}$  and a minimum beam pipe radius  $b=12.5\text{mm}$ .

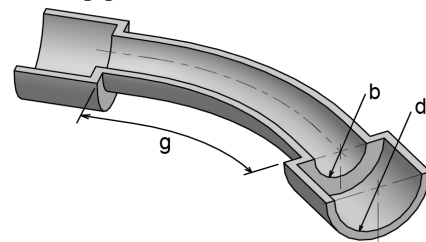


Figure 2: One-quarter of the booster vacuum chamber (arc section).

## Transverse Mode Coupling Instability (TMCI)

Since the step transitions are main contributors to the transverse impedance the TMCI threshold has been

analyzed using results of their geometric and resistive wall impedances. Other vacuum components such as bellows, flanges, valves and etc. were not taken into account.

The geometric kick factor for a step transition has been simulated numerically using the ECHO code. Four stainless steel step transitions with a vertical aperture of  $b=12.5\text{mm}$  and a length of  $g = 31\text{m}$  would produce the kick factor due to the resistive wall  $\kappa_y^{StSt} = 608\text{V/pC/m}$  for  $\sigma_s=4.5\text{mm}$ . With the average vertical betatron function of  $\beta_y = 8.4\text{m}$  these geometries would yield  $\sum \beta_y \kappa_y = 7.2\text{ kV/pC}$ . The threshold current is given by [3]

$$\frac{e^2 N_e^{th} \beta_y}{4 \pi \gamma m c^2 \nu_s} \kappa_y \cong 0.7 \quad (1)$$

where  $N_e^{th}$  is the number of electrons in a bunch at threshold,  $\gamma m c^2$  is the electron energy and  $\nu_s$  is the synchrotron tune. Since the injector accelerates the electrons from 200MeV to 3GeV the threshold current has been estimated at both energies and it corresponds to 4.6mA and 69mA per bunch respectively. The TMCI effect does not significantly limit the single-bunch current and required current 0.28mA per bunch can be accumulated.

### Transverse Coupled Bunch Instability

Higher order modes (Narrow band impedance) and the resistive wall impedance are two main effects limiting high bunch current in many synchrotron facilities. Since many vacuum components are in a design stage the first step is to estimate the transverse coupled bunch instability growth rate in the NSLS-II booster for a stainless steel round vacuum chamber ( $\sigma_{cond} = 1.4 \times 10^6 \text{ S/m}$ ) of length  $L=4 \times g = 124\text{m}$  and beam pipe radius of  $b=12.5\text{mm}$ .

The transverse coupled bunch instability growth rate ( $1/\tau_{gr}$ ) is given by

$$\frac{1}{\tau_{gr}} \cong \frac{e c I_{av} \beta_y}{2 E C} \text{Re} Z_{\perp}^{RW} \frac{1}{\sqrt{1-q}} \quad (2)$$

where  $\text{Re} Z_{\perp}^{RW}$  is the real part of the transverse impedance

$$Z_{\perp}(k) \cong \frac{2}{k b^2} Z_{\parallel}(k), \quad (3)$$

$\beta_y$  is the average value of the betatron function,  $C$  is the booster circumference,  $E$  is the electron energy and  $q$  is the partial number of betatron tune. The longitudinal impedance is given by

$$Z_{\parallel}(k) \cong \frac{(1-i) Z_0 s_0 L}{4 \pi b^2} \sqrt{k s_0} \quad (0 \leq k \ll 1/s_0), \quad (4)$$

where [4],  $s_0 = (2b^2 / Z_0 \sigma_{cond})^{1/3}$ .

The growth time at injection and extraction energies, 200MeV and 3GeV respectively, is shown in Table 2. Since the damping time at injection energy about 21ms

(Fig. 1), the beam is transversely unstable for resistive wall effect. At energy 3GeV radiation damping dominates ( $\tau_D=6\text{ms}$ ) and it stops the transverse coupled bunch instability.

Table 2: The Growth Time at Injection and Extraction Energies.

	200MeV	3GeV
$\tau_{gr}, \text{ms}$	0.8	12
$\tau_D, \text{ms}$	21	6

In order to understand the instability threshold behavior we simulated and compared different effects; including coupled bunch, head-tail, radiation damping and Landau damping. In Figure 3 we show 3D plot of the threshold current dependence as a function of energy and chromaticity. At energies below 2.3GeV the beam is unstable. However our analytical estimate shows that the amplitude of betatron oscillations at energy of 200MeV, is about 1mm. The instability is amplitude limited due to Landau damping from  $\beta$ -tune spread caused by amplitude tune dependence. The amplitude drops down with higher energy. At energies above 2.3GeV the radiation damping dominates and it stops the instability. Based on our simulations we can conclude that observed instability at low energies will not limit the required beam current. The dependence of the threshold on chromaticity is weak. According to analytical estimate, the damping due to head-tail effect is much smaller than the combined adiabatic and radiation damping.

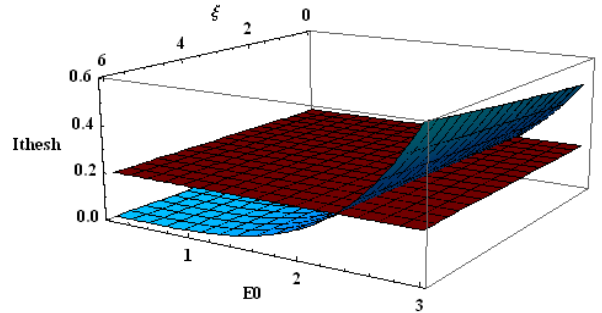


Figure 3: 3D plot of the threshold current as a function of energy and chromaticity.

### Microwave Instability

The threshold condition can be written as [1]

$$I_0^{th} = 9.4 \frac{E V_s^2}{e \alpha (\text{Im} Z / n)_0} (\omega_0 \sigma_{t0})^3 \quad \omega_r \sigma_{t0} \gg 1, \quad (5)$$

where  $E$  is the electron energy,  $V_s$  is the synchrotron tune,  $\alpha$  is momentum compaction,  $\text{Im} Z / n$  is broad band impedance,  $\omega_0$  is revolution frequency,  $\sigma_{t0}$  is bunch duration and  $\omega_r$  is resonant frequency. The instability thresholds per bunch have been estimated at energies 200MeV (30ps) and 3GeV (15ps) they correspond to 2mA and 4mA respectively with the parameters of the

longitudinal broad band impedance  $\text{Im}Z/n=0.5\Omega$  and  $\omega_p=2\pi\times 30\text{GHz}$ .

## ION EFFECTS

NSLS-II injector is designed to deliver high charge per pulse to the storage ring. For the multi-bunch mode operation, 10nC of charge will circulate in the booster ring, distributed in 80 to 150 bunches. Ion trapping and fast-ion instabilities have been analyzed for various filling pattern and total charge [5].

Compared to the storage ring ( $1.3\mu\text{C}$  in 1080 bunches), the booster ring has about 1/100 of circulating charge, but the vacuum pressure will be  $\sim 100$  times higher than the storage ring ( $10^{-7}$  Torr). Thus the ion density from the residual gases is similar. Dominant species of residual gases in the booster ring will be 50%  $\text{H}_2\text{O}$ , 30%  $\text{H}_2$  and 20%  $\text{CO}$ . Ionization cross section can be considered as constant for the electron beam energy from 200MeV to 3GeV.

Ions with atomic mass larger than critical mass will be trapped. The critical mass ( $A_{crit}$ ) was defined by:

$$A_{crit} = \frac{N_b r_p c T_b}{2\sigma_{x,y}(\sigma_x + \sigma_y)} = \frac{N_b r_p L_{sep}}{2\sigma_{x,y}(\sigma_x + \sigma_y)}, \quad (6)$$

where  $N_b$  is number of particles per bunch,  $r_p$  is proton classical radius  $r_p = e^2 / 4\pi\epsilon_0 m_p c^2 \sim 1.5 \times 10^{-18} \text{ m}$ ,  $T_b$  (or  $L_{sep}$ ) is bunch separation and  $\sigma_x, \sigma_y$  the RMS beam size. Due to large beam size and small charges in the bunch, all the ions will be captured in the bunch train of NSLS-II booster ring.

In Fig. 4 we show the ion trapping calculation at various bunches filled in the booster ring, with a total charge of 10nC evenly distributed and average beam size  $400\mu\text{m}/200\mu\text{m}$  (horizontal/vertical). Blue circles in the figure mean ions will be trapped, while green dot is not.

Similarly, with different total charge and bunch train length, the ions might be trapped especially when the total charge is low. Ion frequencies are around 2MHz for  $\text{H}^+$  and 7MHz for  $\text{CO}^+$ . We assume even filling pattern for the calculation. In real machine, bunch-to-bunch current variation will damp the ion effects.

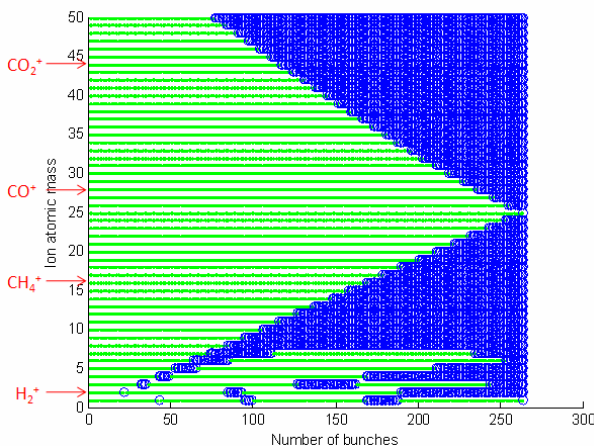


Figure 4: Ion trapping with different bunch train.

Fast ion instability growth rate ( $1/\tau$ ) has been calculated using Stupakov's equation [6]

$$\frac{1}{\tau} \approx \frac{r_e c \beta_y \lambda_{ion}}{3\gamma \sigma_y (\sigma_x + \sigma_y)} \frac{1}{\Delta\omega_i / \omega_i}, \quad (7)$$

where  $\beta_y$  is the vertical beta function, use average  $\beta_y$  value of 10m,  $\Delta\omega_i$  – ion oscillation frequency spread along the ring, taking  $\Delta\omega_i/\omega_i=30\%$  matches the simulation well and  $\lambda_{ion}$  is the ion density defined by:

$$\lambda_{ion} = \frac{n_b N_b}{K_B T} \sigma_{ion} P \quad (8)$$

The fast ion instability growth rate will be  $\sim 3.7\text{ms}$  at the end of bunch train with  $\text{CO}$  partial pressure of  $0.5 \times 10^{-7}$  Torr,  $\text{CO}$  ionization cross section of 2Mbarn, total bunch train charge of 10nC and average beam size  $\sigma_x=400\mu\text{m}/\sigma_y=200\mu\text{m}$ . This is close to the synchrotron radiation damping time at 3GeV of the NSLS-II booster ring. Both normal ion trapping and fast ion instability may become a problem at the booster injection where the damping time is very long.

## CONCLUSION

In this paper we demonstrated that required bunch current is not limited by TMCI and transverse coupled-bunch effects. Predicted transverse coupled-bunch instabilities at energies below 2.3GeV have an amplitude of betatron oscillations about 1mm, that will not drive current reduction.

The longitudinal narrow-band impedance of the vacuum components will be simulated later. We believe that the microwave instability is not an issue for the NSLS-II booster. HOM effect due to cavity structure has been analyzed and presented in a paper by Kawashima [2].

We thank B. Kosciuk for providing us 3D rendering pictures.

## REFERENCES

- [1] NSLS-II Preliminary Design Report, 2008; <http://www.bnl.gov/nsls2/project/PDR/>
- [2] Y. Kawashima and et al., "Instabilities Related with RF Cavity in the Booster Synchrotron for NSLS-II", IPAC2010, Current proceedings.
- [3] S. Krinsky, BNL-75019-2005-IR (2005).
- [4] K.L.F. Bane and M. Sands, SLAC-AP-87 (1991).
- [5] W. Cheng and T. Shaftan, NSLS-II Tech. Note.
- [6] G. Stupakov, Ion effect estimates for the NSLS-II storage ring, NSLS-II tech note.